



## 20 Abstract

21 We illustrate offsets in surface seawater isotopic composition between recent, public  
22 datasets from the Atlantic Ocean and the subtropical southeastern Indian Ocean. The  
23 observed offsets between datasets often exceed 0.10‰ in  $\delta^{18}\text{O}$  and 0.50‰ in  $\delta^2\text{H}$ . They  
24 might in part originate from different sampling of seasonal, interannual or spatial  
25 variability. However, they likely mostly originate from different instrumentations and  
26 protocols used to measure the water samples. Estimation of the systematic offsets is  
27 required before merging the different datasets in order to investigate spatio-temporal  
28 variability of isotopic composition in the world ocean surface waters. This highlights the  
29 need to actively share seawater isotopic composition samples dedicated to specific  
30 intercomparison of data produced in the different laboratories and to promote best  
31 practices, a task to be addressed by the new SCOR working group 171.

32

33

## 34 1. Introduction

35 Seawater isotopic composition ( $^{18}\text{O}/^{16}\text{O}$  and  $^2\text{H}/^1\text{H}$  ratios expressed as  $\delta^{18}\text{O}$  and  $\delta^2\text{H}$  in  
36 ‰ in the VSMOW/SLAP scale) is classified as an Essential Ocean/Climate Variable  
37 (EOV/ECV) in international programs such as GEOTRACES and GO-SHIP. Stable  
38 seawater isotopes ( $\delta^{18}\text{O}$ ,  $\delta^2\text{H}$ ) are used to trace sources of freshwater (precipitation,  
39 evaporation, runoff, melting glaciers, sea ice formation and melting), both at the ocean  
40 surface and in the ocean interior (Schmidt et al., 2007; Hilaire-Marcel et al., 2021).  
41 Except for fractionation during phase changes, the water isotopic composition is nearly  
42 conservative in the ocean.

43 A major emphasis is on high latitude oceanography. There, continental (or iceberg)  
44 glacial melt, formation or melt of sea ice, and high-latitude river inputs (for the Arctic)  
45 leave imprints on the surface ocean isotopic composition, as well as below the surface  
46 down to 800 m close to ice shelves in the Southern Ocean (Randall-Goodwin et al., 2015;  
47 Biddle et al., 2019, Hennig et al., 2024). In contrast, few studies have been performed on  
48 the isotopic signature in the deep ocean (e.g., Prasanna et al., 2015; Voelker et al., 2015).  
49 Seawater isotopes in the upper ocean at low latitudes are often vital for paleoclimatic  
50 studies, as they are needed to calibrate proxies of past ocean variability in marine  
51 carbonate records such as corals and foraminifera (e.g., PAGES CoralHydro2k working  
52 group; Konecky et al., 2020). Seawater isotopes are also important tracers in the coastal  
53 ocean, with emphasis on upwelling (Conroy et al., 2014, 2017; Kubota et al., 2022; Lao et  
54 al., 2022), and river discharges (e.g., Amazon) (Karr and Showers, 2001). Surface ocean  
55 seawater isotopes are also used to characterize evaporation rates and air-sea  
56 interactions (Benetti et al., 2017).

57 The isotopic signatures of these different processes are evolving in our warming world,  
58 which will imprint on the seawater isotopic composition (Oppo et al., 2007).

59 Additionally, seawater isotope data provide model boundary conditions and allow the  
60 assessment of model performance in isotope-enabled Earth system models (e.g. Schmidt  
61 et al., 2007; Brady et al., 2019; Cauquoin et al., 2019), thereby improving climate model  
62 projections of the future.

63 Stable seawater isotope data have thus been massively produced in the last decades by  
64 a variety of methods. For example, most data compiled in the “GISS Global Seawater  
65 Oxygen-18 Database -V1.21” for stable seawater isotopes (LeGrande and Schmidt, 2006)  
66 originate from Isotope-ratio Mass Spectrometry (IRMS). They were mostly measured in  
67 earlier decades by dual-inlet technology (highest precision), whereas, more recently, the  
68 continuous-flow method (lower precision) became widespread for seawater isotope  
69 analysis. In the last decade, cavity ring-down spectroscopy (CRDS) turned into another  
70 commonly used method as it allows parallel measurement of  $\delta^{18}\text{O}$  and  $\delta^2\text{H}$ , but with  
71 often lower precision, at least early on (e.g., Voelker et al., 2015).

72 Reverdin et al. (2022) recently compiled a mix of data produced by IRMS and CRDS at  
73 LOCEAN (<https://www.seanoe.org/data/00600/71186/>). As CRDS and other laser  
74 techniques (Glaubke et al., 2024; hereafter GWS2024) have become more prevalent  
75 recently, they contribute a significant part of the new data produced and thus also to the  
76 soon to be released CoralHydro2k seawater database for  $\delta^{18}\text{O}$  ( $\delta^2\text{H}$ ) with a focus on the  
77 tropics (35°N-35°S) (Atwood et al., 2024).

78 There are potential differences between the data produced by the two methods.  
79 Typically,  $\text{CO}_2$ -water or  $\text{H}_2$ -water equilibration was used for the IRMS measurements  
80 and yields measurements of the activity of water, which decreases with increasing  
81 salinity. Furthermore, concentration of divalent cations like  $\text{Mg}^{++}$  are responsible  
82 for slight changes in fractionation factors. On the other hand, the laser methods such as  
83 CRDS evaporate the entire sample. If the samples have not been distilled beforehand,  
84 there is an issue of salt deposition and of resulting absorption or desorption of water  
85 with fractionation effects. In the LOCEAN database (Reverdin et al., 2022), an attempt  
86 was made to adjust the data, based on the analysis of Benetti et al (2017b). This was also  
87 adopted by at least one other group (Haumann et al., 2022), but overall, there is the  
88 possibility of an offset of these data with respect to the ones of other groups using CRDS.  
89 However, it should be noted that some studies reporting unadjusted  $\delta^{18}\text{O}$  measurements  
90 from CRDS and IRMS technique with  $\text{CO}_2$ -water equilibration provide data that were  
91 undistinguishable within instrumental precision (Walker et al., 2016; Hennig et al.,  
92 2024).

93 It is actually quite common when using water isotope data in studies involving more  
94 than one dataset, to first evaluate whether there are possible offsets. Intercomparison  
95 with earlier data or reference materials was a prerequisite for GEOTRACES sampling  
96 campaigns, although for the water isotopes this was, unfortunately, seldomly followed  
97 (e.g., Voelker et al., 2015). These intercomparisons often outline systematic differences  
98 which could result from the issue outlined above, or from other issues, such as  
99 uncertainties in reference materials used, analysis protocols, or isotopic changes in the  
100 samples during their handling and storage (Benetti et al., 2017a; Akhoudas et al., 2019;  
101 Hennig et al., 2024). In other cases, this was not done, either because the data stood by  
102 themselves (Bonne et al., 2019, for  $\delta^{18}\text{O}$  and  $\delta^2\text{H}$  data), or there was no comparison data  
103 available in the same region (GWS2024, for  $\delta^{18}\text{O}$  data). The possible offsets can however  
104 become an issue, when these data are placed in a larger context. For example, GWS2024  
105 identify a large difference in the S- $\delta^{18}\text{O}$  relationship in the subtropical Indian Ocean  
106 between their data in the southeastern part and other data in the southwestern Indian  
107 Ocean. They also discuss and question differences in the deep water-masses isotopic  
108 values between separate datasets, but as these might also be explained by large  
109 uncertainties in these data, we will not address them further.

110 Using these two examples (Bonne et al., 2019; GWS 2024), the aim of this note is to point  
111 out the interest when producing a new dataset, of exchanging collected samples to carry  
112 a direct comparison, or, if this was not done, to compare the data with other published  
113 data and evaluate potential systematic differences.

## 114 2. Comparisons

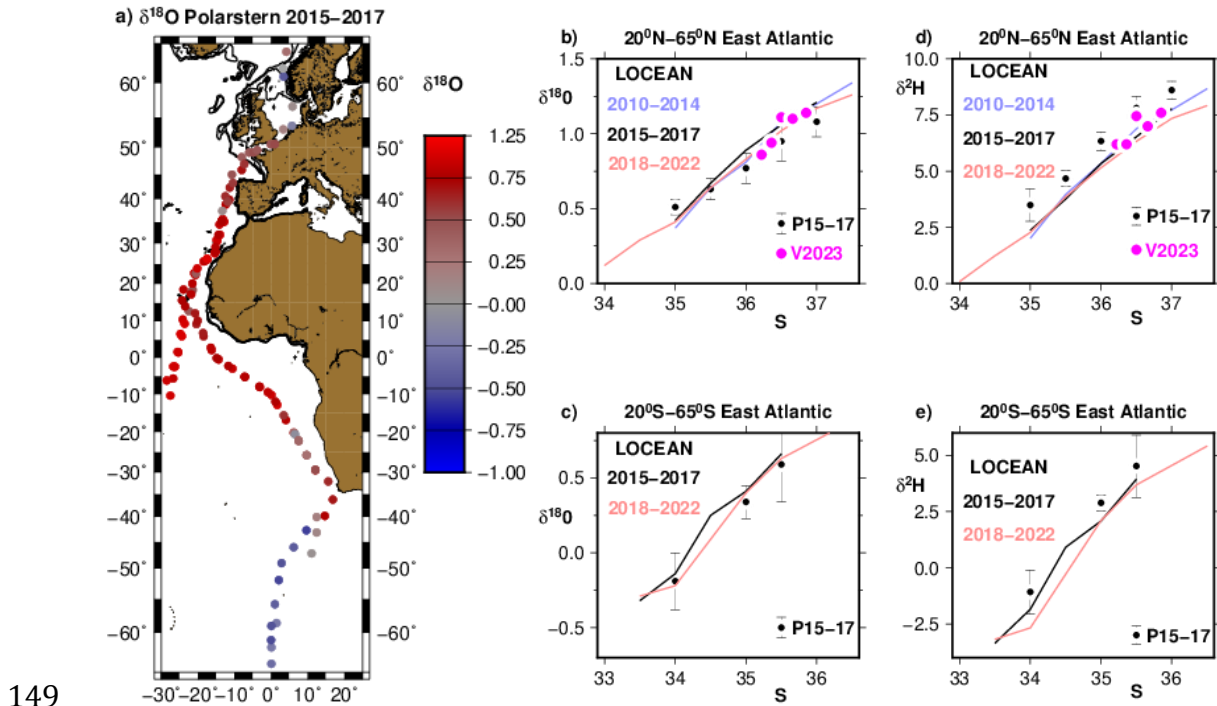
115 For identifying possible offsets, we consider surface ocean subsets of the LOCEAN data  
116 base in specific regions for roughly the same years as the other data collected. The data  
117 extracted are from the same regions as in the datasets of the two studies and are  
118 gathered in S- $\delta^{18}\text{O}$  space as well as in S- $\delta^2\text{H}$  space (only presented for the Bonne et al  
119 (2019) dataset), where S is reported as a practical salinity with the practical salinity  
120 scale of 1978. The assumption done here as in many papers is that the S- $\delta^{18}\text{O}$   
121 relationship holds on fairly large scales in the surface layer (for the eastern subtropical  
122 North Atlantic, see for example, the discussion in Voelker et al (2015) and in Benetti et  
123 al. (2017a)). Obviously, this has limitations, such as in areas influenced by more than

124 one water mass or by multiple freshwater end-members (meteoric, continental run-off,  
125 sea ice melt or formation, evaporation).

## 126 2.1 Daily surface data collected from R.V. Polarstern

127 The surface seawater samples originated from daily collection during two years on  
128 board RV Polarstern in 2015-2017 (Bonne et al., 2019). There is no salinity provided  
129 with the data, and here we chose to associate them with the simultaneously collected  
130 thermosalinograph (TSG) data collected on board the RV Polarstern and available from  
131 PANGAEA (for each cruise, an indexed file with title starting by 'Continuous  
132 thermosalinograph oceanography along Polarstern' is included in PANGAEA: for example,  
133 TSG data for the first cruise (PS90) associated with the isotopic seawater data are found  
134 at <https://doi.org/10.1594/PANGAEA.858885>). The water samples were not collected  
135 from the same water line and pumping depth as the TSG data, which can result in  
136 differences. This is however likely to be small in most circumstances away from large  
137 freshwater input at the sea surface, such as from melting sea ice, intense rainfall and  
138 river estuaries (Boutin et al., 2016). We also applied an adjustment of +0.25‰ to the  
139  $\delta^{18}\text{O}$  data of Bonne et al. (2019), based on post-analysis identification of a bias in an  
140 internal reference material.

141 We then estimate averages of all the data as a function of salinity in two domains  
142 extending poleward of the subtropical salinity maximum toward the higher latitudes in  
143 the eastern part of the Atlantic Ocean (thus, 20°N to 65°N and the same in the southern  
144 hemisphere). This is done by sorting out the data by salinity classes of 0.5. The LOCEAN  
145 data until 2016 in the North and tropical Atlantic were presented by Benetti et al  
146 (2017a), showing the tightness of the S- $\delta^{18}\text{O}$  and S- $\delta^2\text{H}$  relationships in vast domains of  
147 the eastern Atlantic. In the North Atlantic, LOCEAN data have been continuously  
148 collected since 2011, and south of 10°S in the eastern Atlantic mostly since 2017.



149

150 Figure 1: Comparison of the LOCEAN and Bonne et al. (2019) datasets. (a) map of RV  
 151 Polarstern dataset points east of 30°W in the eastern Atlantic Ocean. (b), (c), (d), (e)  
 152 Water isotopes-S scatter diagrams averaged as a function of salinity in 0.5 practical  
 153 salinity bins ((b) and (c) for  $\delta^{18}\text{O}$ ; (d) and (e) for  $\delta^2\text{H}$ ), top for the northern hemisphere  
 154 and bottom for the southern hemisphere, east of 30°W and outside of [20°N, 20°S]. The  
 155 black dots are the binned averages of the Bonne et al. (2019) RV Polarstern data in  
 156 2015-2017 (after adjustment of +0.25‰ to  $\delta^{18}\text{O}$ ) (P15-17), with the root mean square  
 157 of the variance reported as error bars. Five individual surface points from Voelker et al  
 158 (2023) (V2023) are also plotted (magenta dots). The colored lines represent average  
 159 relationships of water isotopes in the LOCEAN data base in the same regions as a  
 160 function of practical salinity for three different period ranges.

161 The average relationships found in the LOCEAN dataset for three periods overlay well in  
 162 particular in the northern hemisphere. Uncertainties on individual curves (not shown)  
 163 are estimated based on the scatter of individual data in each salinity bin. They are  
 164 typically on the order of 0.01-0.02 (0.05-0.10) ‰ for  $\delta^{18}\text{O}$  ( $\delta^2\text{H}$ ) respectively in the  
 165 northern hemisphere (top panel), and a little larger for the less sampled southern  
 166 hemisphere curves in 2015-2017. Sampling is usually also insufficient at the low end of  
 167 the salinity range, to reliably estimate an uncertainty. Thus, these different curves nearly  
 168 overlay within the sampling uncertainty. Five surface samples that were collected in the

169 Northeast Atlantic during the same years within the same salinity range (Voelker et al.,  
170 2023), also fit well on the North Atlantic curves. The adjusted  $\delta^{18}\text{O}$  data from Bonne et  
171 al. (2019) are slightly shifted downward with respect to the curves (Fig. 1b, c), with the  
172 plotted standard deviation of individual data around the average not overlapping the  
173 LOCEAN data average curves in most cases for the same years 2015-2017. The situation  
174 is opposite for the 35-salinity bin in the northern hemisphere, with the adjusted  $\delta^{18}\text{O}$   
175 data from Bonne et al. (2019) being above the three LOCEAN average curves, which  
176 might be due to samples collected uniquely in the English Channel and North Sea by RV  
177 Polarstern in this salinity range, whereas sampling is more geographically-spread in the  
178 LOCEAN data base.

179 Altogether, the average  $\delta^{18}\text{O}$  offset is small, with the LOCEAN data being higher by  $0.02 \pm$   
180  $0.01 \text{ ‰}$  than the  $\delta^{18}\text{O}$  from Bonne et al. (2019), which is not significantly different from  
181 0 based on the interannual differences witnessed in the LOCEAN curves and the  
182 scatter/uncertainty in the RV Polarstern data. A systematic difference is, however, found  
183 for  $\delta^2\text{H}$ , with LOCEAN data been lower than  $\delta^2\text{H}$  from Bonne et al. (2019) by  $0.99 \pm$   
184  $0.07 \text{ ‰}$  (Fig. 1d, e).

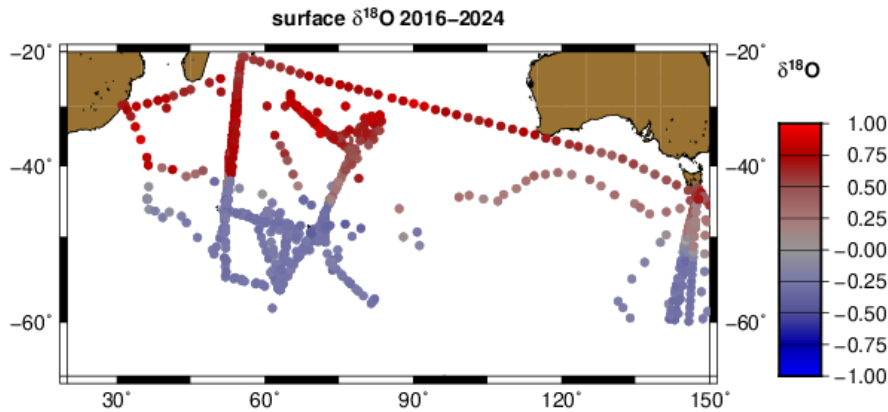
185

## 186 2.2 Southern subtropical Indian Ocean

187 GWS2024 describe a synthesis of water isotope data in the southern Indian Ocean  
188 combining their data collected in 2018 in the southeastern Indian Ocean (CROCCA-2S)  
189 with earlier data in the southwestern Indian Ocean, in particular from LOCEAN, as well  
190 as data from the southern Australian shelf collected mostly in 2010 (Richardson et al.,  
191 2019), and in the equatorial Indian Ocean (Kim et al., 2021). In the most recent version  
192 of the LOCEAN dataset, in addition to data included by GWS2024 and collected mostly  
193 west of  $80^\circ\text{E}$ , there are two transects with surface data through the southeastern Indian  
194 Ocean, one collected in February 2017, and the other in March 2024, thus in mid to late  
195 austral summer. These transects cross the region covered by the CROCCA-2S dataset,  
196 albeit not close to western Australia, as well as the area of the Richardson et al. (2019)  
197 dataset, south of Australia. The LOCEAN dataset also contains surface data south of  
198 Tasmania (in 2017, as well as in 2020 to 2024). All these data correspond to samples



199 analyzed on a CRDS Picarro L2130 at LOCEAN, and with the protocols discussed by  
 200 Reverdin et al. (2022). The bottles in which the samples were stored were the same ones  
 201 for most of the samples, and time between collection and analysis varied, but was mostly  
 202 on the order of 6 months or less. Thus, this is a homogeneously produced set of data for  
 203 the years 2016-2024, which spatially and temporally overlaps with the data used by  
 204 GWS2024 collected south of Australia and in the southeastern Indian Ocean (Fig. 2).

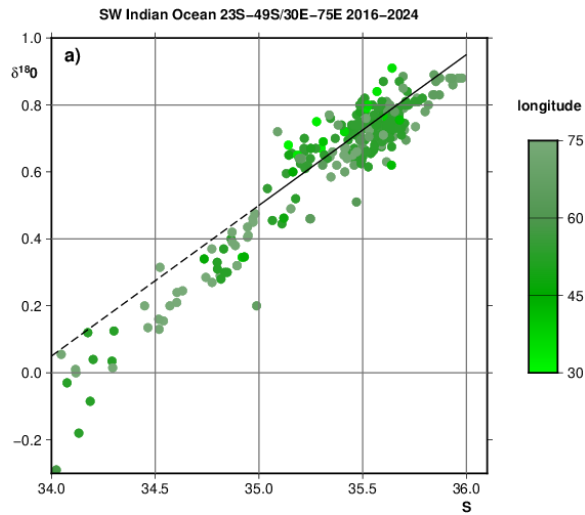


205  
 206

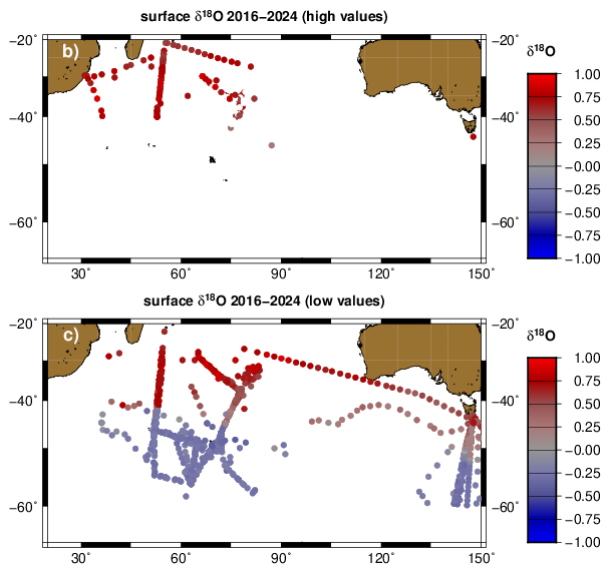
207 Figure 2: Map of  $\delta^{18}\text{O}$  surface data in the LOCEAN archive for 2016-2024, north of 60°S.  
 208 All data are associated with S and  $\delta^2\text{H}$  measurements.

209 The LOCEAN data distribution plotted in the  $S\delta^{18}\text{O}$  space presents a wide  $\delta^{18}\text{O}$  range at a  
 210 given salinity in the southwestern Indian Ocean (Fig. 3a) for S between 35 and 36. For  
 211 this range which covers a large part of the surface water of the southwestern Indian  
 212 Ocean's subtropical gyre, we establish a regression line for the LOCEAN  $\delta^{18}\text{O}$  as a  
 213 function of S, which can be seen as a mixing line. Above this line, there are no data points  
 214 for lower S (Fig. 3a), with data at higher S found north of 28°S as well as in the far  
 215 southwestern Indian Ocean, but with some remnants found all the way to the core of the  
 216 subtropical gyre near 75°E/35°S (Fig. 3b). Data below the regression line contain most  
 217 of the data east of 60°E for latitudes south of 28°S and connect the salinity maximum  
 218 region with the lower salinity south of the Subtropical Front and down to the region  
 219 south of the Polar Front (Fig. 3c). These subtropical lower isotopic values in  $S\delta^{18}\text{O}$   
 220 space, which already appear in part of the repeated (1998-2024) French OISO cruises  
 221 data at 50°E, dominate east of 60°E.

222



223

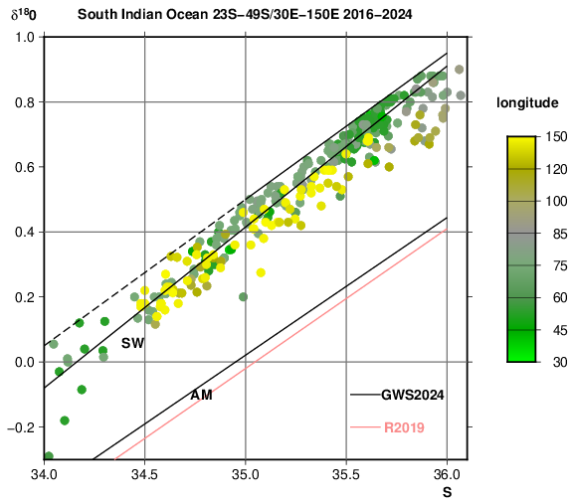


224

225 Figure 3: (a)  $S$ - $\delta^{18}\text{O}$  scatter diagram of 0-30m LOCEAN data within the southwestern  
 226 region (30-75°E/23-49°S) coloured as a function of longitude, with the regression line  
 227 (black line) of the data in  $S$ - $\delta^{18}\text{O}$  space for the 35-36 range in practical salinity. The  
 228 spatial distributions of the LOCEAN data with higher and lower  $\delta^{18}\text{O}$  relative to that  
 229 regression line in the whole Indian Ocean north of 60°S are shown on panels (b) and (c),  
 230 respectively.

231 We will now focus on the lower part of the distribution in  $S$ - $\delta^{18}\text{O}$  space (Fig. 3c), which  
 232 overlaps with the location of the data from CROCCA-2S and the near-Australia data from  
 233 GWS2024 (the higher values in Fig. 3c do not). For salinities above 35 one observes a

234 lowering of  $\delta^{18}\text{O}$  at given salinity from  $50^\circ\text{E}$  in the western Indian Ocean to at least  
 235  $100^\circ\text{E}$  (Fig. 4) with more stable values further east. This lowering is on the order of 0.15  
 236 at most, even for the higher salinities (35.5 or more) for which it is strongest.



237

238 Figure 4:  $S$ - $\delta^{18}\text{O}$  scatter plot of 0-30m LOCEAN Indian Ocean data as shown in Fig. 3c,  
 239 color-coded as a function of longitude, below the partially stippled regression line for  
 240 the SW Indian Ocean (reproduced from Fig. 3a). The two black lines correspond to the  
 241 two linear relationships (GWS2024) for the 0-100m layer between  $23^\circ\text{S}$  and  $49^\circ\text{S}$  for the  
 242 south-west Indian Ocean (SW) and for the Australian margin south of Australia (AM)  
 243 (we use the original relation of  $\delta^{18}\text{O} = 0.4231 * S - 14.7876$ , instead of the rounded-up  
 244 relation reported in the paper; R. H. Glaubke, pers. comm., 2024), and the pink line is the  
 245 earlier linear relationship for the 0-600m layer along the Australian margin by  
 246 Richardson et al. (2019) (R2019).

247 Thus, besides some gradual and smaller changes, we do not observe in the LOCEAN  
 248 surface dataset a large sudden change in the  $S$ - $\delta^{18}\text{O}$  distribution near  $75^\circ\text{E}$  or  $85^\circ\text{E}$   
 249 between the southeastern and southwestern Indian Ocean, nor a further strong change  
 250 closer to the Australian coastal margin, as suggested by figures 6 and 7 of GWS2024.  
 251 Most of the LOCEAN  $S$ - $\delta^{18}\text{O}$  data south of  $28^\circ\text{S}$  correspond to the mixing of a low salinity  
 252 end-member characteristic of the fresh waters of the Southern Ocean (at  $S < 34$ ) with  
 253 waters which are imprinted by air-sea exchange in the subtropical gyre at higher  
 254 salinities up to 36 and more, as discussed by GWS2024. These LOCEAN ( $S$ ,  $\delta^{18}\text{O}$ ) values  
 255 are significantly above the linear relationships proposed by GWS2024 (based on their  
 256 figures 5a, 6 and 7). This positive offset at given  $S$  seems to be about 0.05-0.10 ‰ in the

257 southwestern Indian Ocean, but close to 0.50 ‰ for the Australian coastal margins,  
258 although we could not access the individual data of R2019 for that latter region. These  
259 offsets are much larger than the spread in the LOCEAN data, which is on the order of  
260 0.10 ‰. Furthermore, the LOCEAN data support the presence of a secondary low  
261 salinity end member at  $S < 35$  with heavier isotopic composition, contributing to the  
262 water-mass properties in the far southwestern Indian Ocean as well as for the area  
263 sampled between 20°S and 28°S north of the subtropical salinity maximum. This could  
264 be a contribution of the Indonesian Through Flow and tropical western Indian Ocean  
265 surface waters, as discussed by Kim et al. (2021) and GWS2024. We could not carry out  
266 a comparable comparison for  $\delta^2\text{H}$  which is not presented by GWS2024, and which  
267 exhibits a too large spread in the CROCCA-2S dataset to reach a firm conclusion.

### 268 3. Discussion

269 In the two intercomparisons of surface data presented in this note, we find significant  
270 differences between datasets. Do these differences originate from spatio-temporal  
271 variability or from systematic offsets between the different datasets?

272 In the case of the RV Polarstern dataset (Bonne et al., 2019), an error in a specified  
273 reference material value was found after the publication, and the adjusted data present  
274 only a small, non-significant  $\delta^{18}\text{O}$  negative offset, but a significant positive  $\delta^2\text{H}$  offset  
275 with respect to LOCEAN data. Differences might arise from spatial differences. For  
276 example, in the northern hemisphere, values at salinity close to 35 mostly originate from  
277 the North Sea and English Channel in the RV Polarstern dataset, thus with more mid-  
278 latitude continental influence than for most of the LOCEAN data in the same salinity  
279 range which have a contribution of more depleted subpolar and polar freshwater. One  
280 expects a larger isotopic range in the South Atlantic for salinities less than 35, due to  
281 intermittent presence of sea ice or iceberg melt, and at higher salinities due to the  
282 presence of different water masses originating from the South Atlantic and southeastern  
283 Indian Ocean. However, the current dataset is not sufficient to estimate it.

284 Furthermore, different seasons were sampled in the two datasets. In the northeastern  
285 Atlantic sector, Bonne et al. (2019) surface data east of 30°W were collected in April and  
286 November north of 10°S and in November south of 10°S in the southeastern Atlantic.

287 These data do not suggest large seasonal differences in the Northeast Atlantic,  
288 concurring with the LOCEAN S- $\delta^{18}\text{O}$  data in the tropics to mid-latitudes (20 to 50°N),  
289 which are tightly distributed along a mean S- $\delta^{18}\text{O}$  relationship, and thus with low  
290 seasonal variability of this relationship (Benetti et al., 2017a; Voelker et al., 2015). The  
291 LOCEAN data are not numerous enough in the southeastern Atlantic to further evaluate  
292 whether the offset is constant throughout the dataset, or presents a component related  
293 to geographical temporal or spatial variability.

294 To investigate the South Indian Ocean seawater isotopic composition, GWS2024  
295 combined datasets that were processed in different laboratories. Potential offsets  
296 between those could thus cause apparent spatial variability. In particular, GWS2024  
297 outline large spatial contrasts in the S- $\delta^{18}\text{O}$  relationship across the surface subtropical  
298 Indian Ocean and southern Australia that are at least a factor two smaller in the recent  
299 version of the LOCEAN dataset.

300 Seasonal or interannual variability might contribute to the differences shown on Fig. 3,  
301 as the data in the southeastern Indian Ocean from GWS2024 were collected in  
302 November-December, whereas the data in the LOCEAN database in this region are  
303 mostly from February-March. However, at least south of Tasmania, where the LOCEAN  
304 dataset also contains December data, it does not seem that the seasonal cycle causes  
305 changes larger than 0.05 ‰ at the same salinity. A difference due to seasonality would  
306 thus be barely identifiable in that case, noting the possible presence of interannual  
307 variability and that the long-term accuracy in the analyses in some centers, such as AWI  
308 Potsdam and LOCEAN, is 0.05 ‰. Richardson et al. (2019) also commented that south of  
309 Australia there was little difference between a southern winter cruise and late summer  
310 (March) data. Further west, near 55-70°E, earlier surface data in the OISO surveys, as  
311 well as the vertical upper profiles of OISO station data also suggest a rather modest  
312 seasonal variability on the order of 0.10 ‰. Changes could also arise from interannual  
313 variability, but the range of interannual variability in the LOCEAN data base is smaller  
314 than the difference between the GWS2024 curves for the southeastern Indian Ocean and  
315 south of Australia and the corresponding LOCEAN data. Thus, a likely cause of the large  
316 differences between the South Indian Ocean/Australia margin data combined in the  
317 GWS2024 study is the existence of systematic offsets between the data produced by  
318 different institutes.

## 319 4. Conclusions

320 What these two comparisons suggest is that offsets are present between different recent  
321 published datasets, which exceed 0.10 ‰ in  $\delta^{18}\text{O}$  and 0.50 ‰ in  $\delta^2\text{H}$ , thus larger than  
322 the target long-term accuracy of analyses in individual isotopic laboratories. Moreover,  
323 errors in reference material values are always possible and require post-analysis  
324 intercomparisons, such as the one that led to the correction of the RV Polarstern dataset  
325 (Bonne et al., 2019). Furthermore, one contribution to a systematic difference between  
326 the LOCEAN dataset and data from other institutes is that the LOCEAN data are reported  
327 in ‘freshwater’ concentration scale (Benetti et al., 2017b). The use of this concentration  
328 scale corrects possible effects of salt in the water activity measured by IRMS with  $\text{CO}_2$ -  
329 equilibration and the effect of salt accumulation during evaporation in laser  
330 spectroscopy, which both can lead to fractionation, possibly of similar magnitude  
331 (Walker et al., 2016). Different comparisons based on duplicates collected during cruises  
332 suggest that this is a main cause of difference between LOCEAN data and other datasets  
333 (LOCEAN  $\delta^{18}\text{O}$  data being more positive). Poor conservation of the samples during  
334 storage, analytical protocols, or uncertainties in the specified values of reference  
335 material are other sources of differences between data produced in different institutes.

336 Different methods have been used for intercomparing and detecting systematic offsets  
337 between different datasets. One common approach is to compare values obtained in  
338 specific water masses, for which we expect little variability of the water isotopic  
339 composition. This is often attempted, but data density is often limited, and the resulting  
340 uncertainties are difficult to assess. Datasets with intermediate and deep data in the  
341 Southern Ocean might be valuable to systematically test this approach, and model-based  
342 reconstructions of isotopic composition of sea water could also be incorporated.

343

344 An alternative, in particular for the surface data, is to develop approaches based on the  
345 systematic comparison of nearby data in space and time. In some ways, the assumption  
346 behind this and what was done in the mapping by LeGrande and Schmidt (2006), that is  
347 that the bulk of the variability is from large scale relationships of water isotopes and  
348 salinity. This is also what has been done by crossover analyses in major geochemical  
349 databases, such as GLODAP, with an attempt to adjust offsets for  $\delta^{13}\text{C}$ -DIC with a similar  
350 low-density data distribution in the North Atlantic (Becker et al., 2016). The comparison

351 presented here (Fig. 1) of the S-water isotopes surface distribution in the North and  
352 South Atlantic of the LOCEAN and the RV Polarstern (Bonne et al., 2019) datasets  
353 suggests that this can be used to estimate offsets. Required improvements, in particular  
354 for estimating uncertainties would be to take into account estimates of seasonal,  
355 interannual and spatial variability in these relationships. However, this requires that  
356 there are enough overlapping data within regions of relatively homogeneous water  
357 masses, or some independent estimates on these signals, for example from model  
358 simulations.

359

360 As the spatial and temporal data density is often reduced, we expect that the  
361 uncertainties in estimated offsets will be large. This could reduce the usefulness of the  
362 isotopic data for different oceanographic and climate studies, with large uncertainties in  
363 estimated S- $\delta^{18}\text{O}$  (or S- $\delta^2\text{H}$ ) relationships to validate proxies used for paleo-climate  
364 reconstructions, or for identifying emerging climate-change related signals.

365

366 Scientific Committee of Oceanic Research (SCOR) working group 171 MASIS (Towards  
367 best practices for Measuring and Archiving Stable Isotopes in Seawater) has recently  
368 been established to contribute tackling these issues, both for water isotopes and the  
369 isotopic composition of inorganic carbon in sea water,  $\delta^{13}\text{C}$ -DIC. For that, it aims to  
370 actively involve the international community in establishing guidelines for data  
371 production (collection, storage, measurement) and quality control, as well as for  
372 validating the data and comparing well-documented archived data originating from  
373 different laboratories. It will review the methods to estimate errors and offsets between  
374 the different datasets. An important step for this effort is to directly intercompare  
375 measurements by the different laboratories of shared well-preserved water samples  
376 distributed quickly, as had earlier been done for  $\delta^{13}\text{C}$ -DIC (Cheng et al., 2019). This,  
377 together with enhancing interaction within the scientific community needs to be actively  
378 pursued, in order to reduce the errors when merging different datasets and increase the  
379 potential use of the water isotope data.

380

381 Data availability

382 The LOCEAN data are available at <https://www.seanoe.org/data/00600/71186/>.

383 The isotopic data of the Bonne et al. (2019) are available as indicated in the paper, with  
384 here S added from the PANGAEA archive, as described in the text. The GWS2024 data  
385 are available as described in the paper. However, among the data used in this paper, we  
386 could not access the data from the Richardson et al. (2019) paper.

387

388 Author contribution: GR initiated the study and prepared the manuscript with  
389 contributions from all coauthors. AV initiated the intercomparison effort, and AV, CW,  
390 and HM contributed to editing the paper. HM was also responsible from producing the  
391 data in the Bonne et al. (2019) paper.

392

393 Competing interests: The authors declare that they have no conflict of interest.

394

395 Acknowledgments

396 The LOCEAN isotopic laboratory is supported by OSU Ecce Terra of Sorbonne Université.  
397 We are thankful to Catherine Pierre and Jérôme Demange who have set and help run the  
398 facility, and for Aïcha Naamar, Marion Benetti and Camille Akhoudas to have measured  
399 some of the water samples. We are grateful for support by INSU, Nicolas Metzl and Claire  
400 Lo Monaco for samples during the OISO cruises on RV MD2, by IPEV during the SOCISSE  
401 program on RV Astrolabe, with on board support by Patrice Bretel and Rémi Foletto, and  
402 by IPSL for supporting the LOCEAN data base and intercomparisons. Antje Voelker  
403 thanks Joanna Waniek (IOW, Germany) for collecting the NE Atlantic water samples and  
404 Robert van Geldern (GeoZentrum Nordbayern, Germany) for analyzing them. AV also  
405 acknowledges financial support by Fundação para a Ciência e a Tecnologia (FCT) through  
406 projects Centro de Ciências do Mar do Algarve (CCMAR) basic funding  
407 UIDB/04326/2020 (<https://doi.org/10.54499/UIDB/04326/2020>) and programmatic  
408 funding UIDP/04326/2020 (<https://doi.org/10.54499/UIDP/04326/2020>) and the  
409 CIMAR associated laboratory funding LA/P/0101/2020  
410 (<https://doi.org/10.54499/LA/P/0101/2020>). The RV Polarstern dataset was funded  
411 by the AWI Strategy Fund Project ISOARC. Comments by Alexander Haumann (AWI) and  
412 by two anonymous reviewers were very helpful.

413

414 References



- 415 Aoki, S., Kobayashi, R., Rintoul, S. R., et al.: Changes in water properties and flow regime  
416 on the continental shelf off the Adélie/George V Land coast, East Antarctica, after glacier  
417 tongue calving, *J. Geophys. Res.: Oceans*, 122, 6277-6294, 2017.
- 418 Akhoudas, C. H., Sallée, J.-B., Haumann, F. A., Meredith, M. P., Garabato, A. N., Reverdin, G.,  
419 Jullion, L., Aloisi, G., Benetti, M., Leng, M. J., and Arrowsmith, C.: Ventilation of the abyss  
420 in the Atlantic sector of the Southern Ocean, *Nature scientific reports*, **11**, 16733,  
421 <https://doi.org/10.1038/s41598-021-95949-w>, 2020, 2021.
- 422 Atwood, A. R., Moore, A.L., Long, S., Pauly, R., DeLong, K., Wagner, A., and Hargreaves, J.A.:  
423 The CoralHydro2k Seawater  $\delta^{18}\text{O}$  Database, *Past Global Changes Magazine* 32,59, doi:  
424 10.22498/pages.32.1.59, 2024.
- 425 Becker, M., Andersen, N., Erlenkeuser, H., Tanhua, T., Humphreys, M.P., and Körtzinger, A.:  
426 An Internally Consistent Dataset of  $\delta^{13}\text{C}$ -DIC Data in the North Atlantic Ocean. *Earth Sys.*  
427 *Sci. Data*, 8, 559-570, doi: 10.5194/essd-8-559-2016, 2016.
- 428 Benetti, M., Reverdin, G., Aloisi, G., and Sveinbjörnsdóttir, A.: Stable isotopes in surface  
429 waters of the Atlantic Ocean: indicators of ocean-atmosphere water fluxes and oceanic  
430 mixing processes. *J. Geophys. Res. Oceans*, doi:10.1002/2017JC012712, 2017a.
- 431 Benetti, M., Sveinbjörnsdóttir, A. E., Ólafsdóttir, R., Leng, M. J., Arrowsmith, C., Debondt,  
432 K., Fripiat, F., and Aloisi, G.: Inter-comparison of salt effect correction for  $\delta^{18}\text{O}$  and  $\delta^2\text{H}$   
433 measurements in seawater by CRDS and IRMS using the gas-H<sub>2</sub>O equilibration method,  
434 *Marine chemistry*, doi:10.1016/j.marchem.2017.05.010, 2017b.
- 435 Biddle, L. C., Loose, B., and Heywood, K. J.: Upper ocean distribution of glacial meltwater  
436 in the Amundsen Sea, Antarctica. *J. Geophys. Res. Oceans*, 10.1029/2019JC015133. et al.,  
437 2019.
- 438 Bonne, J.-L., Behrens, M. Meyer, H., Kipfstuhl, S., Rabe, B., Schönicke, L., Steen-Larsen, H.  
439 C., Werner, M.: Resolving the controls of water vapour isotopes in the Atlantic sector.  
440 *Nature Comm.* 10, 1632, doi: 10.1038/s41467-019-09242-6, 2017.
- 441 Boutin, J., Chao, Y., Asher, W. E., Delcroix, T., Drucker, D., et al.: Satellite and In Situ  
442 Salinity: Understanding Near-Surface Stratification and Subfootprint Variability. *Bull. of*  
443 *the Amer. Meteor. Soc.*, 97 (8), pp.1391-1407. 10.1175/BAMS-D-15-00032.1, 2016.
- 444 Brady, E., Stevenson, S., Bailey, D., Liu, Z., Noone, D., Nusbaumer, J., Otto-Bliesner, B. L.,  
445 Tabor, C., Thomas, R., Wong, T., Zhang, J., Zhu, J.: The connected isotopic water cycle in

- 446 the Community Earth System Model Version 1, *J. Adv. Model. Earth Syst.*, 11, 8,  
447 <https://doi.org/10.1029/2019MS001663>, 2019.
- 448 Cauquoin, A., Werner, M., Lohmann, G.: Water isotopes – climate relationships for the  
449 mid-holocene and preindustrial period simulated with an isotope-enabled version of  
450 MPI-ESM, *Clim. Past* 15, 1913-1937, <https://doi.org/10.5194/cp-15-1913-2019>, 2019.
- 451 Cheng, L., Normandeau, C., Bowden, R., Doucett, R., Gallagher, B., Gillikin, D. P.,  
452 Kumamoto, Y., McKay, J. L., Middlestead, P., Ninnemann, U., Nothaft, D., Dubinina, E. O.,  
453 Quay, P., Reverdin, G., Shirai, K., Mørkved, P. T., Theiling, B.P., van Geldern, R., and  
454 Wallace, D. W. R.: An international intercomparison of stable carbon isotope  
455 composition measurements of dissolved inorganic carbon in seawater, *Limnology and*  
456 *Oceanography: Methods* 17, 200-209, <https://doi.org/10.1002/lom3.10300>, 2019.
- 457 Glaubke, R. H., Wagner, A., and Sikes, E. L.: Characterizing the stable oxygen isotopic  
458 composition of the southeast Indian Ocean, *Marine Chemistry*, 262,  
459 <https://doi.org/10.1016/j.marchem.2024.104397>, 2024.
- 460 Haumann, F. A. et al.: [Data set], Zenodo, doi:10.5281/zenodo.1494915, 2019.
- 461 Hennig, A., Mucciarone, D. A., Jacobs, S. S., Mortlock, R. A., and Dunbar, R. B.: Meteoric  
462 water and glacial meltwater in the southeastern Amundsen Sea: a time series from 1994  
463 to 2020, *The cryosphere*, 18, 791-818, <https://doi.org/10.519/tc-18-791-2024>, 2024.
- 464 Hilaire-Marcel, C., Kim, S. T., Landais, A., Ghosh, P., Assonov, S., Lécuyer, C., Blanchard, M.,  
465 Meijer, H. A., and Steen-Larsen, H. C.: A stable isotope toolbox for water and inorganic  
466 carbon cycle studies, *Nature Reviews Earth & Environment* 2 (10), 699-719, 2021.
- 467 Kim, Y., Rho, T., and Kang, D.-J.: Oxygen isotope composition of seawater and salinity in  
468 the western Indian Ocean: Implications for water mass mixing, *Mar. Chem.* 237, 104035,  
469 <https://doi.org/10.1016/j.marchem.2021.104035>, 2021.
- 470 Konecky, B. L. et al.: The Iso2k database: a global compilation of paleo- $\delta^{18}\text{O}$  and  $\delta^2\text{H}$   
471 records to aid understanding of Common Era climate, *Earth Syst. Sci. Data*, 12, 2261–  
472 2288, <https://doi.org/10.5194/essd-12-2261-2020>, 2020.
- 473 Kumar, P. K., Singh, A., and Ramesh, R.: Convective mixing and transport of the Bay of  
474 Bengal water stir the  $\delta^{18}\text{O}$ -salinity relation in the Arabian Sea., *J. Mar. Sys.* 238, 103842,  
475 <https://doi.org/10.1016/j.jmarsys.2022.103842>, 2023.

- 476 LeGrande, A. N. and Schmidt, G. A.: Global gridded data set of the oxygen isotopic  
477 composition in seawater, *Geophys. Res. Lett.* 33,  
478 <https://doi.org/10.1029/2006gl026011>, 2006.
- 479 Oppo, D. W., Schmidt, G. A., and LeGrande, A. N.: Seawater isotope constraints on tropical  
480 hydrology during the Holocene, *Geophys. Res. Lett.* 34, L13701,  
481 <https://doi.org/10.1029/2007GL030017>, 2007.
- 482 Randall-Goodwin, E., Meredith, M. P., Jenkins, A., Yager, P. L., Sherrell, R. M., Abrahamsen,  
483 E. P., Guerrero, R., Yuan, X., Mortlock, R. A., Gavahan, K., Alderkamp, A.-C., Ducklow, H.,  
484 Robertson, R., and Stammerjohn, S. E.: Freshwater distributions and water mass  
485 structure in the Amundsen Sea polynya region, Antarctica. *Elementa: Science of the*  
486 *Anthropocene*, 3: 000065, <https://doi.org/10.12952/journal.elementa.000065>, 2015.  
487 et al., 2015.
- 488 Reverdin, G., et al.: The CISE-LOCEAN sea water isotopic database (1998-2021), *Earth*  
489 *sci. sys. data*, <https://doi.org/10.5194/essd-2022-34>, 2022.
- 490 Richardson, L. E., Middleton, J. F., Kyser, T. K., James, N. P., and Opdyke, B. N.: Shallow  
491 water masses and their connectivity along the southern Australian continental margin,  
492 *Deep Sea Res. I, Oceanogr. Res. Pap.* 152, 103083,  
493 <http://doi.org/10.1016/j.dsr.2019.103083>, 2019.
- 494 Schmidt, G. A., LeGrande, A. N., and Hoffmann, G.: Water isotope expressions of intrinsic  
495 and forced variability in a coupled ocean-atmosphere model, *J. Geophys. Res.* 112,  
496 D10103, <https://doi.org/10.1029/2006jd007781>, 2007.
- 497 Voelker, A., Colman, A., Olack, G., Waniek, J. J., and Hodell, D.: Oxygen and hydrogen  
498 isotope signatures of Northeast Atlantic water masses, *Deep-Sea Res. II*, 116, 89-106.  
499 <https://doi.org/10.1016/j.dsr2.2014.11.006>, 2015.
- 500 Voelker, A. H.: Seawater oxygen and hydrogen stable isotope data from the upper water  
501 column in the North Atlantic Ocean (unpublished data). *Interdisciplinary Earth Data*  
502 *Alliance (IEDA)*, <https://doi.org/10.26022/IEDA/112743>, 2023.
- 503 Walker, S. A., Azetsu-Scott, K., Normandeau, C., Kelly, D. E., Friedrich, R., Newton, R.,  
504 Schlosser, P., McKay, J. L. Abdi, W., Kerrigan, E., Craig, S. E., and Wallace, D. W. R.: Oxygen  
505 isotope measurement of seawater ( $\text{H}_2^{18}\text{O}/\text{H}_2^{16}\text{O}$ ). A comparison of cavity ring-down  
506 spectroscopy (CRDS) and isotope ratio mass spectrometry (IRMS), *Limnol. and*  
507 *Oceanography: Methods*, 14, 31-38, <https://doi.org/10.1002/lom3.10067>, 2016.